# Organization of chromatin and histone modifications at a transcription site

Waltraud G. Müller,[1] Dietmar Rieder,[2] Tatiana S. Karpova,[1] Sam John,[1] Zlatko Trajanoski,[2] and James G. McNally[1]

[1]Laboratory of Receptor Biology and Gene Expression, National Cancer Institute, Bethesda, MD 20892
[2]Christian Doppler Laboratory for Genomics and Bioinformatics, Institute for Genomics and Bioinformatics, Graz University of Technology, 8010 Graz, Austria

According to the transcription factory model, localized transcription sites composed of immobilized polymerase molecules transcribe chromatin by reeling it through the transcription site and extruding it to form a surrounding domain of recently transcribed decondensed chromatin. Although transcription sites have been identified in various cells, surrounding domains of recently transcribed decondensed chromatin have not. We report evidence that transcription sites associated with a tandem gene array in mouse cells are indeed surrounded by or adjacent to a domain of decondensed chromatin composed of sequences from the gene array. Formation of this decondensed domain requires transcription and topoisomerase IIα activity. The decondensed domain is enriched for the trimethyl H3K36 mark that is associated with recently transcribed chromatin in yeast and several mammalian systems. Consistent with this, chromatin immunoprecipitation demonstrates a comparable enrichment of this mark in transcribed sequences at the tandem gene array. These results provide new support for the pol II factory model, in which an immobilized polymerase molecule extrudes decondensed, transcribed sequences into its surroundings.

## Introduction

There is increasing evidence for a spatial organization of transcription (Iborra and Cook, 2002; Chakalova et al., 2005). Pol II molecules form clusters within cells (Iborra et al., 1996), and nascent transcripts accumulate there, defining these clusters as transcription sites (Jackson et al., 1993; Wansink et al., 1996). These transcription sites can transcribe different genes from distant parts of the same chromosome or potentially even different chromosomes (Osborne et al., 2004).

According to the transcription factory model (Cook, 1999), transcription sites contain immobilized pol II molecules that spool the chromatin template in and out of the site. To date, however, evidence for movement of the chromatin template through a transcription site is largely theoretical. It has been argued that because transcripts appear within a restricted volume defining the transcription site, the polymerase cannot move very far, and so it is more likely that the chromatin template moves (Cook, 1999). This scenario also solves entanglement problems of the transcript and template (Cook, 1999).

If the chromatin template is reeled in and out of a transcription site, this site should be adjacent to or surrounded by decondensed, transcribed chromatin. In fact, transcription sites are surrounded by chromatin (Iborra et al., 1996), but, because most structures in the nucleus are found within chromatin, it has not been clear whether the chromatin seen around any one transcription site is associated with loci being transcribed by that site.

To investigate the spatial organization of chromatin at a transcription site, we have taken advantage of a mouse cell line harboring a tandem array. The array is composed of 200 directly repeated copies of a 9-kb element composed of the mouse mammary tumor virus (MMTV) promoter followed by reporter gene sequences (Walker et al., 1999).

Transcription from the array can be induced above basal levels by a hormone-stimulated GFP-tagged glucocorticoid receptor (GR) that also enables visualization of the array in live or fixed cells (McNally et al., 2000). Hormone induces a transcriptional response at the array comparable with that at single-copy MMTV promoters, including the recruitment of cofactors (Müller et al., 2001), specific nucleosome remodeling (Fragoso et al., 1998), and adaptation to prolonged hormone treatment (Fragoso et al., 1998). In addition, higher order chromatin structures at the array are indistinguishable from the structures observed in transcriptionally active domains of natural chromosomes (Müller et al., 2004).

Therefore, the array exhibits several features that are characteristic of normal transcription. Because of its size, however, the array is readily detected by light microscopy. Thus, it provides a useful model system for examining in a single cell the

Correspondence to James G. McNally: mcnallyj@exchange.nih.gov

Abbreviations used in this paper: BrUTP, bromo-UTP; ChIP, chromatin immunoprecipitation; GR, glucocorticoid receptor; MMTV, mouse mammary tumor virus.

The online version of this article contains supplemental material.

The Journal of Cell Biology, Vol. 177, No. 6, June 18, 2007 957–967
http://www.jcb.org/cgi/doi/10.1083/jcb.200703157

spatial distribution of molecules associated with a transcriptionally active locus to construct a more unified picture of the nuclear organization of both these molecules and the chromatin at a transcription site. Using this approach, we report evidence for a previously undetected spatial organization at a transcription site, namely a domain of decondensed chromatin that borders or surrounds the transcription sites and appears likely to contain recently transcribed chromatin.

## Results

### Transcription sites and active pol II associate with the array and interdigitate between GFP-GR beads

We examined the location of transcription sites at the array by first using bromo-UTP (BrUTP) incorporation for detection of nascent transcripts. This consistently yielded a series of BrUTP puncta associated with the GFP-GR–tagged array (Fig. 1, a and b). As previously described, the array itself is composed of GFP-GR puncta or beads (Müller et al., 2004). To ascertain whether the BrUTP puncta overlaid the GFP-GR beads, we performed 3D deconvolution for improved resolution, including corrections for residual chromatic aberration along the optical axis. We consistently found that the BrUTP puncta did not directly colocalize with the GFP-GR beads but rather interdigitated between the beads, with some overlap at the edges of these two distributions (Fig. 1, c and d). These observations are consistent with earlier studies suggesting that transcription occurs predominantly at or near the surface of compact chromatin domains, namely in the interchromatin or perichromatin domains (Cmarko et al., 1999; Verschure et al., 1999).

Because the BrUTP incorporation procedure involves live cell permeabilization that might conceivably alter the relative distribution of transcription sites and GFP-GR beads, we used an alternate approach to address the same question. Fixed cells were probed with an antibody (H5) against the phosphorylated CTD domain of pol II to determine its association with GFP-GR at the array. This likewise yielded a punctate staining pattern for active pol II that was clearly enriched at the array (Fig. 1, e and f). This punctate pol II staining pattern is consistent with live cell images from a previous study that examined a GFP-tagged pol II in the array cell line (Becker et al., 2002). Again, using 3D deconvolution for improved resolution, we found that the active pol II, like the BrUTP incorporation sites, did not directly colocalize with the GFP-GR beads but interdigitated between them (Fig. 1, g and h).

Finally, we analyzed the degree of overlap between the active pol II and the BrUTP stains at the array and found a high degree of colocalization (Fig. 1, i–l). These observations identify the BrUTP puncta as transcription factories and are consistent with previous studies demonstrating transcription foci in various cell types (Jackson et al., 1993; Wansink et al., 1996). The pol II factories that we detected are larger than typical pol II factories but comparable in size with pol I factories (Hozak et al., 1994). This similarity in size may reflect the fact that the pol I factories also associate with a tandem array (in this case, of ribosomal genes). In summary, these results establish that the transcription sites at the array are located directly adjacent to the GFP-GR beads, with some overlap at the edges between these two distributions.

### Decondensed chromatin from the MMTV array surrounds or is adjacent to the pol II transcription sites

It has been proposed that loops of highly decondensed chromatin extrude from transcription sites (Cook, 1995). If so, at the resolution afforded by light microscopy, each transcription site

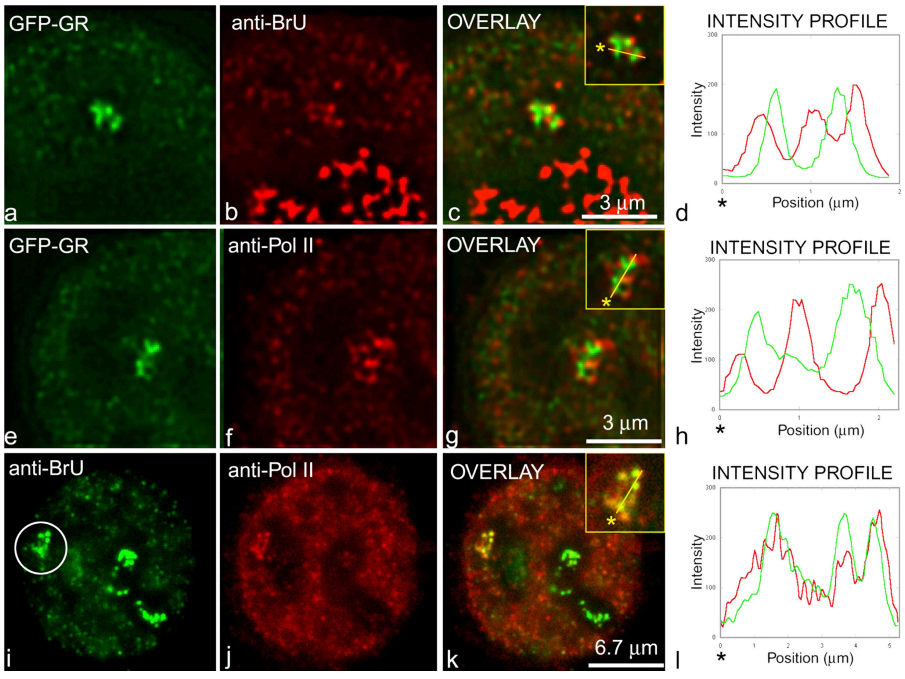


Figure 1. **Transcription sites interdigitate between GFP-GR beads.** (a–h) Transcription sites were visualized either by BrUTP incorporation followed by antibody detection of BrUTP (a–c) or by using an antibody against the active form of pol II (e–g). Images in a–c and e–g were deconvolved and corrected for chromatic aberration. Transcription sites at the array (b and f) are displaced from the GFP-GR beads, with occasional overlap at the edges of these distributions (c and g). Insets in c and g show the path starting at the asterisk over which red and green intensities were measured (d and h). (i and j) As a consistency check, triple-label analysis was performed using GFP-GR (not depicted) to identify the location of the array (circle in i), and immunofluorescence was performed with antibodies against BrUTP (i) and active pol II (j). (k and l) The antibody stains overlap considerably. The inset in k shows the path starting at the asterisk over which red and green intensities were measured (l). Note that as expected, pol I transcriptional activity in the nucleolus is marked by intense BrUTP incorporation (b and i). Because BrUTP levels in nucleoli are considerably higher than at the array, the nucleolar incorporation is saturated in these images to optimize visualization of the array signal.

at the array should be associated with a domain of decondensed chromatin. However, our previous DNA FISH experiments suggested that array chromatin exactly coincides with the GFP-GR beads (Fig. S1, available at http://www.jcb.org/cgi/content/full/jcb.200703157/DC1; Müller et al., 2001). This GFP-GR bead chromatin could, in principle, correspond to the predicted decondensed domain, but our previous estimates suggest it is considerably more condensed than expected for transcribed chromatin (Müller et al., 2001).

We reasoned that if additional, more decondensed chromatin was associated with transcription sites at the array, its fragility might make it difficult to preserve by our earlier procedure of DNA FISH with denaturation at 95°C (Müller et al., 2001). Thus, we performed DNA FISH at a lower denaturation temperature (70°C) and compared the results to DNA FISH with denaturation at 95°C. At 95°C, we once again detected beaded structures identical to those we had previously observed (Fig. 2 a). However, with denaturation at 70°C, we could also detect specific MMTV-labeled chromatin structures in every cell (Fig. 2 b). These structures contained some puncta that resembled the beads seen at 95°C, but the structures seen at 70°C also exhibited a haze interspersed between the puncta that was not as evident at 95°C. Furthermore, direct measurement of areas encompassed by the structures demonstrated that those detected at 70°C were significantly larger ($P < 10^{-6}$) than those detected at 95°C (Fig. 2 c). The 70°C structures were never detected in control experiments in which the specific DNA probe was omitted, although staining of the nuclear periphery and random spots within the nucleus was still apparent (Fig. S2 a, available at http://www.jcb.org/cgi/content/full/jcb.200703157/DC1). All of the specific structures detected by these two FISH protocols contain DNA, as an RNase treatment is always included in the DNA FISH procedures, and both the 70 and 95°C structures were eliminated by pretreating cells with DNase (unpublished data).

To determine whether there was any overlap between the DNA detected by the 70 and 95°C procedures, we devised a dual-temperature DNA FISH protocol that involved FISH at 70°C with a red-labeled probe followed by an additional fixation step to ensure preservation of the 70°C structure and FISH at 95°C with a green-labeled probe. This dual FISH procedure consistently enabled the preservation and detection of two distinct structures that showed virtually no overlap between the red (70°C) and green (95°C) labels in all cells (Fig. 2, d–i). This observation suggests that the 70 and 95°C structures are largely exclusive. Observation of many cells with the dual FISH procedure showed that the 70°C (red) structure typically surrounded the 95°C (green) structure (Fig. 2, d–f), although in a few cells, the 70°C (red) structure protruded largely from one side of the 95°C (green) structure (Fig. 2, g–i).

We also investigated whether we could reverse the preceding dual DNA FISH procedure; that is, we performed FISH first at 95°C and then at 70°C. In this reverse procedure, the decondensed domain was no longer detected (Fig. S2 b). This suggests that the chromatin within this domain is fragile and easily destroyed by 95°C treatment unless it is extensively prefixed.

The fragility of the 70°C structure suggests that it is more decondensed than the 95°C structure. Consistent with this, we found that the mean FISH intensity per unit area was approximately sevenfold higher in the 95 vs. 70°C structures, suggesting a considerable increase in DNA concentration within the GFP-GR beads relative to the decondensed domain. Note that

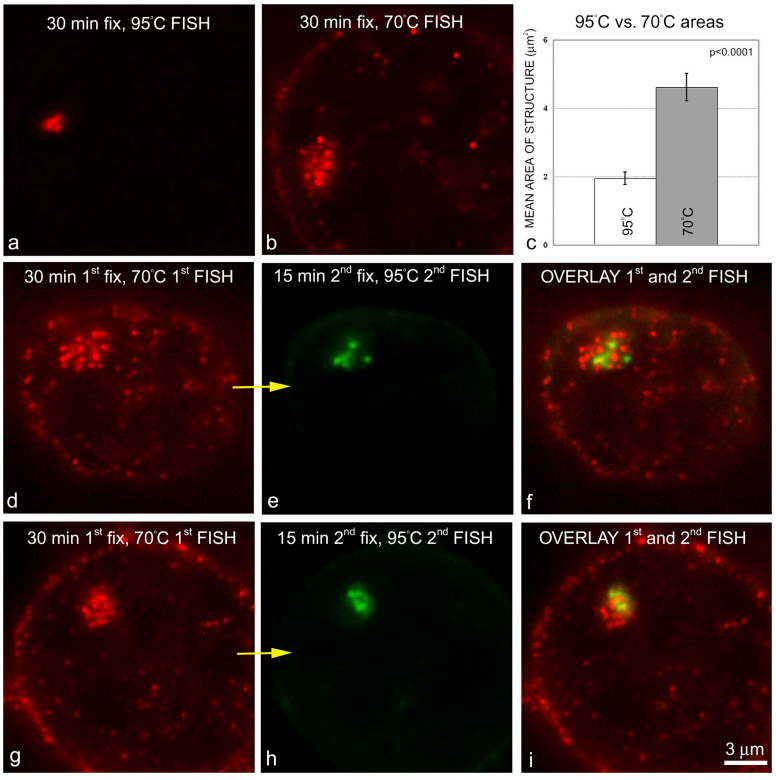


Figure 2. **Distinct array-specific structures are detected by DNA FISH at different denaturation temperatures.** (a) As previously reported (Müller et al., 2001, 2004), structures can be detected by DNA FISH with denaturation at 95°C that overlap the GFP-GR beads (Fig. S1, available at http://www.jcb.org/cgi/content/full/jcb.200703157/DC1). (b and c) However, with denaturation at 70°C (b), much larger structures are detected (c). (d–i) These 70 and 95°C structures are distinct and can be detected reproducibly in all cells using a double FISH protocol. Here, denaturation is first performed at 70°C, and the denatured DNA is labeled with a red probe (d and g). (e and h) This is followed by an additional fixation step (arrows) to preserve the more fragile 70°C structure, denaturation at 95°C, and the newly denatured DNA labeled with a green probe. (f and i) Double-label imaging of these cells demonstrates that in most cells, the 70°C structure surrounds the 95°C structure (f), although, occasionally, the 70°C structure extends largely to one side of the 95°C structure (i). Based on the fragility and estimated DNA density of the 70°C structure, we refer to it as the decondensed domain. Based on its overlap with the GFP-GR stain, we refer to the 95°C structure as either the GFP-GR beads or condensed domain. Error bars represent SEM.

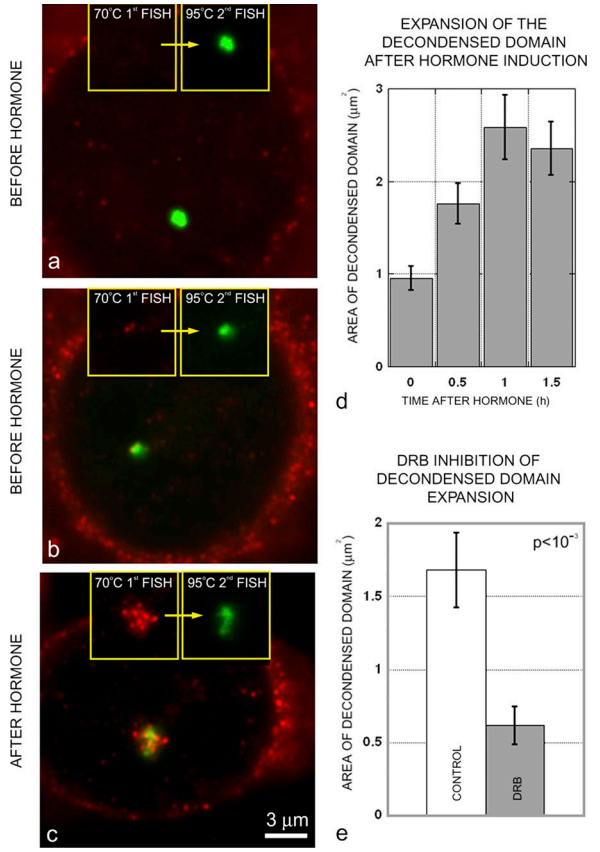


Figure 3. **The decondensed domain markedly expands upon transcriptional activation, and this expansion is inhibited by DRB.** (a and b) Consistent with low levels of basal expression from the MMTV promoter, decondensed domains were either absent (a) or very small (b) in cells before hormone addition. (c) Much larger decondensed domains were present 1.5 h after hormone addition. (a–c) The overlay images of the double FISH procedure are shown, with the insets showing separately the first (70°C; red) followed by (arrows) the second (95°C; green) steps of the double FISH. Areas of the decondensed domains were measured by thresholding the edge of the structure. (d and e) The mean area increased over time after hormone induction of transcription (d), but this increase could be significantly reduced ($P < 10^{-3}$) by the drug DRB, which prevents pol II elongation (e). Error bars represent SEM.

this is a rough approximation because the measurements were made in 2D instead of 3D and because of the possibility that the 70 and 95°C FISH protocols may have different efficiencies of DNA preservation or hybridization.

We conclude that there are two chromatin compartments at the array: a more condensed domain that corresponds directly to the GFP-GR beads surrounded by or adjacent to a more decondensed domain detectable only by lower temperature DNA FISH.

## Formation of the decondensed domain requires transcription and topoisomerase IIα activity

We next investigated whether the decondensed domain arose as a result of transcription. To test this, we measured areas of the decondensed domain detected by DNA FISH at 70°C as a function of time before and after transcriptional activation by hormone induction. Before activation and consistent with the known low levels of basal transcription from the MMTV promoter (Toohey et al., 1990), small decondensed domains were visible in some cells, whereas in other cells, none could be detected (Fig. 3, a and b). In contrast, a single chromatin bead could always be detected by DNA FISH at 95°C, marking the site of the condensed array (Fig. 3, a and b). After activation, decondensed domains were present in every cell (Fig. 3 c), and their mean area increased substantially over time (Fig. 3 d).

As a second test of the decondensed domain's association with transcription, we induced transcription by the addition of hormone but simultaneously added a transcriptional inhibitor, DRB (5,6-dichloro-1-β-D-ribobenzimidazole; Chodosh et al., 1989). This significantly inhibited ($P < 10^{-3}$) formation of the decondensed domain (Fig. 3 e), also suggesting that formation of this domain is coupled to transcription.

As another test for the possible involvement of the decondensed domain in transcription, we investigated its association with a topoisomerase. Transcription generates positive supercoils in front of a polymerase and negative supercoils behind it (Liu and Wang, 1987). If not relieved by topoisomerase action, the resultant torsional strain may accumulate to levels that could stall transcription (Mondal et al., 2003).

We stained the array cell line with two different antibodies against topoisomerase IIα. For each antibody, we detected a similar association pattern with the array: a region of topoisomerase IIα staining extended around and beyond the GFP-GR beads (Fig. 4, a–c).

To determine the relationship of the topoisomerase IIα staining pattern with the decondensed domain, we performed immuno-FISH and found that the topoisomerase II stain and the decondensed domain consistently overlapped (Fig. 4, d–f). These results suggest that topoisomerase IIα associates with the decondensed domain and may perform some function there.

To test this, we inhibited topoisomerase IIα using the drug etoposide. We found that formation of the decondensed domain was impaired (Fig. 4 g) compared with controls in which cells were treated with vehicle only. As detected by RNA FISH, etoposide treatment also sharply reduced transcription from the array compared with the controls (Fig. 4 h). These results indicate that transcription sites at the array are associated with a surrounding region of topoisomerase IIα that is required both for transcription from the array and for formation of the decondensed domain around the array.

## The decondensed domain is enriched in trimethyl H3K36, a histone mark characteristic of recent transcription

Several studies in both yeast and mammals have demonstrated that histones in recently transcribed chromatin are marked with a trimethyl H3K36 modification (Bernstein et al., 2005; Morris et al., 2005; Pokholok et al., 2005; Vakoc et al., 2006). We reasoned that if the decondensed domain contains recently transcribed chromatin extruded from the pol II factories, it should show increased levels of trimethyl H3K36.

To determine whether this mark was associated with transcribed chromatin from the MMTV array, we performed chromatin immunoprecipitation (ChIP) using an antibody specific for trimethyl H3K36 and compared the levels of this mark

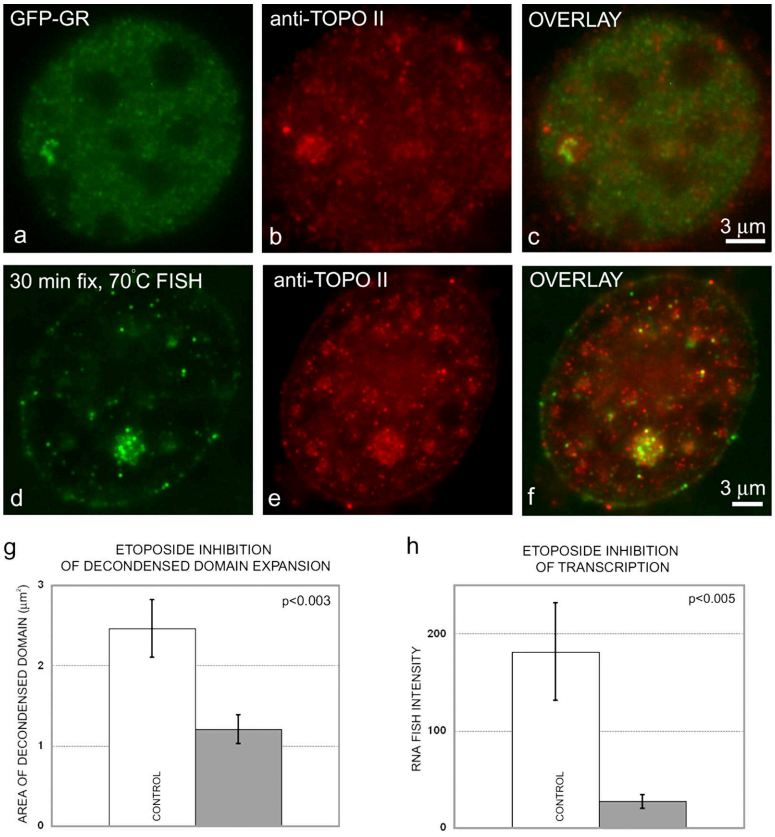


Figure 4. **Topoisomerase IIα associates with the decondensed domain and is required for expansion of the decondensed domain.** (a–c) Immunofluorescence reveals that topoisomerase IIα is distributed in a domain surrounding the GFP-GR–tagged array. (d–f) An immuno-FISH procedure demonstrates that the topoisomerase IIα stain colocalizes with the decondensed domain. (g) Expansion of the decondensed domain upon transcriptional activation is inhibited by etoposide. (h) As detected by RNA FISH intensity measurements, etoposide also dramatically reduces transcription from the array. Error bars represent SEM.

within the MMTV promoter to the downstream ras reporter gene. Consistent with previous studies of other genes (Bernstein et al., 2005; Morris et al., 2005; Pokholok et al., 2005; Vakoc et al., 2006), we found that compared with the MMTV promoter, the reporter gene sequence exhibited a substantial enrichment for the trimethyl H3K36 mark. This differential effect was enhanced upon the hormone induction of transcription but was still detected to a lesser degree without hormone (Fig. 5 a), which is consistent with basal transcription from the MMTV promoter (Toohey et al., 1990) and with our unpublished observations of RNA FISH accumulation at the array in the absence of hormone.

With this evidence for trimethyl H3K36 enhancement in the transcribed reporter gene sequence, we proceeded to examine the distribution of this mark at the MMTV array by confocal microscopy. Immunofluorescence with the same trimethyl H3K36 antibody used for ChIP revealed a staining pattern that surrounded the GFP-GR beads (Fig. 5, b–d). To follow up this observation, we also performed immunofluorescence with an antibody against the N terminus of the human huntingtin-interacting protein B (HYPB), which possesses H3K36 histone methyltransferase activity (Sun et al., 2005) and is an orthologue of the Set2 methyltransferase responsible for the H3K36 trimethylation mark in yeast (Strahl et al., 2002). This HYPB antibody also exhibited a staining pattern that surrounded the array (Fig. 5, e–g), suggesting that the trimethyl H3K36 mark itself as well as an enzyme potentially responsible for it were associated with the decondensed domain.

In contrast, strikingly different staining patterns were observed in confocal images of antibodies directed against histone marks typically associated with active promoters and 5′ regions (Liang et al., 2004; Schneider et al., 2004; Bernstein et al., 2005; Pokholok et al., 2005; Roh et al., 2005). Of the three antibodies tested (generically acetylated H4, trimethyl H3K4, and acetyl H3K9), all stained the condensed chromatin domain, yielding substantial colocalization with the GFP-GR beads, but showed little or no stain of the decondensed domain (Fig. 6).

The enhanced staining of the GFP-GR beads by antibodies specific for active promoters could reflect a preferential retention of 5′ sequences in the condensed domain compared with the decondensed domain or, alternatively, could reflect the fact that there is likely to be considerably more chromatin within the condensed domain compared with the decondensed domain (approximately seven times more based on our rough estimates; see Decondensed chromatin from the MMTV array…).

To distinguish between these possibilities, we performed DNA FISH at both 70 and 95°C with a probe for the MMTV promoter sequence. These FISH experiments revealed that this sequence was present in both the condensed (95°C FISH) and decondensed (70°C FISH) domains (Fig. 7, a, b, and e–g). Thus, promoter sequences do not appear to be preferentially retained within the condensed domain. Consequently, the enhancement of active promoter marks and GFP-GR staining in the condensed domain most likely reflects the increased chromatin concentration there.

We then repeated these probe-specific FISH experiments, but with a probe for the ras reporter gene sequence. Here, as for

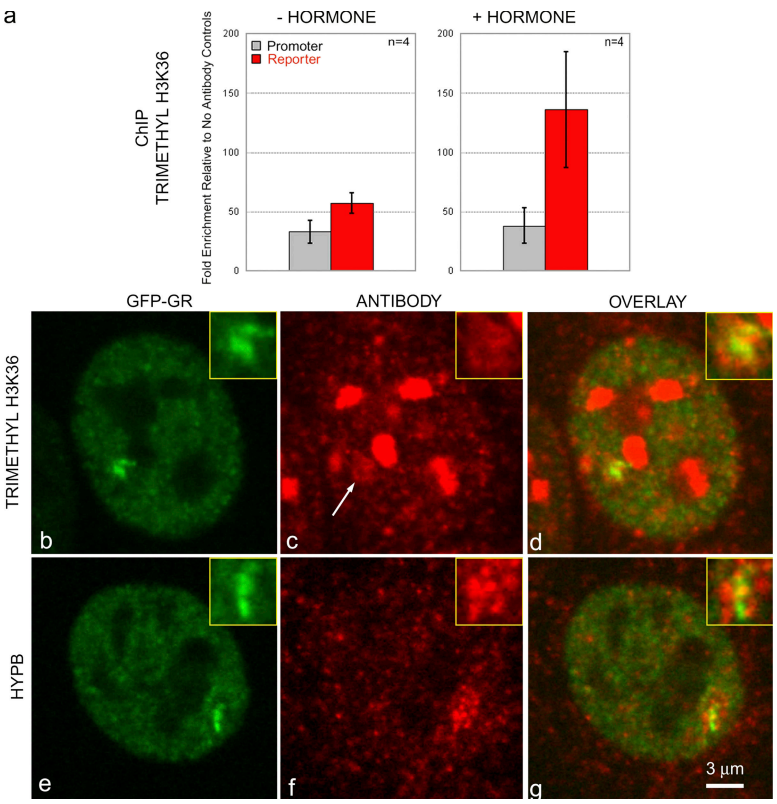


Figure 5. **A histone modification associated with transcribed regions is found in the decondensed domain.** Consistent with published studies of other genes in yeast and mammalian systems, ChIP reveals that the trimethyl H3K36 histone mark is enhanced in the transcribed region of the array relative to the promoter. (a) Transcribed region, red bars; promoter, gray bars. The mean fold enrichments with SEM (error bars) are shown from four separate chromatin isolations with and without hormone induction. Before hormone treatment (−hormone), some enhancement of the trimethyl H3K36 mark was reproducibly seen in the reporter relative to the promoter. After hormone treatment (+hormone), the enhancement of the trimethyl H3K36 mark in the reporter increased substantially in all experiments. (b–d) Immunofluorescence with the same trimethyl H3K36 antibody yields by confocal microscopy an enhanced stain (arrow in c) that surrounds the GFP-GR beads (b–d; with higher magnification views in the insets), suggesting that this is the domain containing recently transcribed sequences from the array. Note that a darker footprint corresponding to the location of the GFP-GR beads is present in the trimethyl H3K36 stain (compare insets in b and c), suggesting that this mark is largely excluded from the beads even though there is much more chromatin there. Also note that the trimethyl H3K36 antibody yields intense staining of nucleoli. This might conceivably reflect transcribed rDNA sequences, although there are no reports to date of whether transcribed pol I genes are also marked in this way. (e–g) An antibody against a histone methyltransferase thought to be responsible for the H3K36 methylation mark (HYPB, a Set2 orthologue) also stains a region surrounding the GFP-GR beads, but no comparable staining is seen in nucleoli, suggesting that another methyltransferase might be responsible for the H3K36 staining within nucleoli.

the promoter sequences, we could also detect reporter sequences in both the condensed and decondensed domains (Fig. 7, c, d, and h–j). Thus, despite both the increased chromatin concentration and the presence of reporter gene sequences in the condensed domain, staining for the trimethyl H3K36 mark is not enhanced in the condensed GFP-GR beads but rather only in the decondensed domain. Because the trimethyl H3K36 mark labels recently transcribed chromatin, this result argues (1) that the reporter gene sequences in the condensed domain have not yet been transcribed and (2) that as these sequences are transcribed, they appear in the decondensed domain.

## Discussion

### Overview

Structural analysis of transcriptionally active chromatin is challenging as a result of difficulties in identifying, preserving, and resolving the structures at such sites. We have overcome some of these limitations in this study by developing a new protocol for DNA FISH and applying it to a tandem gene array that is easily visualized by light microscopy. With these tools, we have now identified three different structures at the array that provide new insights into how transcription may occur there (Fig. 8). First, as we previously described (Müller et al., 2004), we find a series of adjacent puncta or beads of relatively condensed chromatin that can be identified by either conventional DNA FISH or in live or fixed cells by the accumulation of GFP-GR. Second, directly adjacent to this condensed domain, we find transcription sites identified by either BrUTP incorporation or by an antibody against the active form of pol II. Third, we find that these transcription sites are surrounded by and contained within a larger domain that is composed of more decondensed chromatin from the array. As explained below, our results suggest that this decondensed domain arises from the extrusion of transcribed sequences from an immobilized polymerase, providing new support to the pol II factory model of transcription.

### Structural evidence for a decondensed domain

Some hints for chromatin-surrounding transcription sites had previously come from electron microscopy sections of HeLa cells in which transcription sites were detected by biotinylated RNA, and the presence of chromatin surrounding them was inferred by a uranyl-EDTA regressive staining technique (Iborra et al., 1996). Because this procedure detects all transcription sites and all chromatin, some amount of interpretation was required to imagine where the associated chromatin might begin and end for each transcription site or even whether the chromatin adjacent to a transcription site was composed of DNA associated with that site.

Our new evidence for a decondensed chromatin domain surrounding transcription sites at the array is more direct and substantial. Using a specially developed, gentler DNA FISH protocol, we were able to detect decondensed, array-specific chromatin extending to a clear boundary around only the transcription sites associated with the array. This demonstrates that a specific set of transcription sites is surrounded by a decondensed chromatin domain composed of sequences from the loci being transcribed. It seems likely that we and others have missed such decondensed domains before by DNA FISH

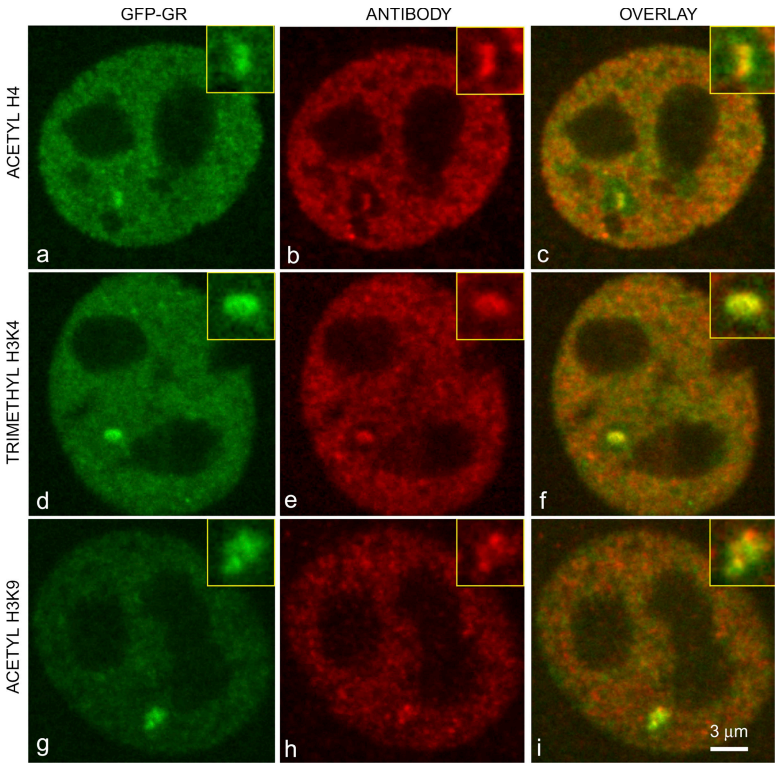


Figure 6. **The GFP-GR beads colocalize with histone modifications that are typically associated with promoters and the 5′ regions of transcribed genes.** Confocal microscope images show GFP-GR (green) and immunofluorescent images (red) with antibodies against generically acetylated H4 (a–c), trimethyl H3K4 (d–f), and acetyl H3K9 (g–i). Insets show higher magnification views of the array.

because they are difficult to preserve, are normally composed of a variety of different DNA sequences dependent on the genes being transcribed at the transcription site (Osborne et al., 2004), and are likely to be much smaller for a transcription site associated with single-copy genes of moderate transcriptional activity.

According to the simplest form of the pol II factory model, the decondensed domain surrounding a transcription site should be composed of loops of decondensed chromatin. Our light microscopy images cannot resolve such structures, but our DNA FISH detection procedure yields a punctate staining pattern in the decondensed domain that might reflect a more complex structural organization there. However, given the fragility of the chromatin within this domain, some alteration of fine structure might be expected after the fixation and denaturation procedures used to detect it. A live cell marker for the decondensed domain (analogous to GFP-GR for the beads) will be necessary to draw any firm conclusions with light microscopy about the substructure of this domain.

### Evidence for involvement of the decondensed domain in transcription

We made several observations linking the array's decondensed domain with transcription. DRB treatment, which blocks transcriptional elongation (Chodosh et al., 1989), hinders formation of the decondensed domain, suggesting that transcriptional elongation is required for the formation of the decondensed domain. We also found that topoisomerase IIα associates with the decondensed domain and so is poised to remove supercoils that would arise on either side of a transcribing polymerase (Liu and Wang, 1987). Inhibition of topoisomerase II function by a brief (45 min) drug treatment impaired formation of the decondensed domain and dramatically reduced transcription. Both effects could arise if the drug treatment blocked the elongation of pol II either as a result of accumulated torsional strain or immobilized topoisomerase complexes, although effects of topoisomerase inhibition on promoter activation are also possible (Collins et al., 2001).

More direct molecular evidence for the role of the decondensed domain in elongation comes from the presence within the decondensed domain of a marker, trimethyl H3K36, which is characteristically found at multiple sites along transcribed genes (Bannister et al., 2005; Morris et al., 2005; Pokholok et al., 2005; Vakoc et al., 2006). Indeed, we found by ChIP that the trimethyl H3K36 mark is enhanced in the transcribed reporter sequences of the array compared with the promoter sequence. This indicates that when used in immunofluorescence, the same trimethyl H3K36 antibody should reveal the location and distribution of transcribed sequences at the array. This antibody stained a region that surrounded and extended well beyond the GFP-GR beads, suggesting that chromatin within the decondensed domain was recently transcribed. However, the BrUTP incorporation experiments demonstrate that transcription occurs only at the transcription sites directly adjacent to the GFP-GR beads (Fig. 1). Thus, it appears that transcribed sequences from the array do not remain at the transcription sites but instead are extruded into the surroundings, giving rise to the decondensed domain (Fig. 2).

The trimethyl H3K36 mark was unique among the histone modifications that we tested because it was the only one that showed enhanced staining that surrounded the GFP-GR beads. In contrast, active promoter marks instead showed enhancement

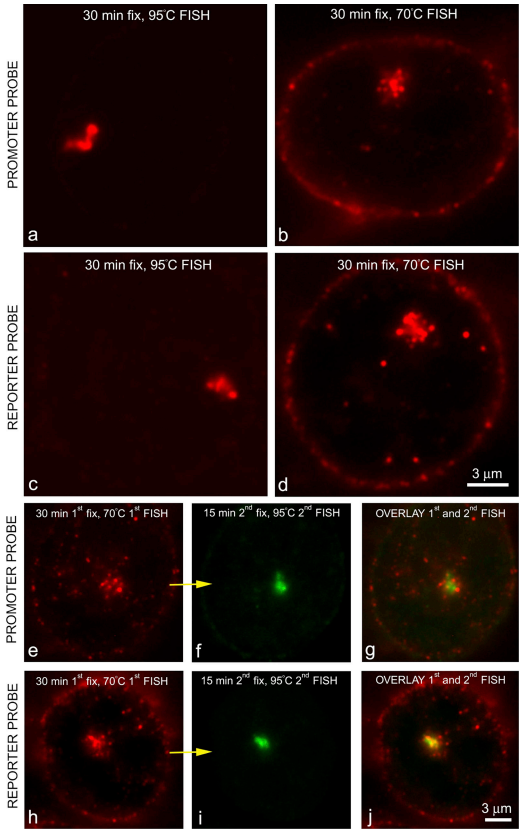


Figure 7. **Promoter and reporter sequences are present in both the condensed and decondensed domains.** Similar condensed (95°C FISH; a and c) and decondensed (70°C FISH; b and d) domain structures are detected with DNA probes specific for either the array's MMTV promoter (a and b) or ras reporter gene (c and d). (e–j) The same is true when the double FISH procedure is used, demonstrating that promoter and reporter sequences are present in both the condensed and decondensed domains. Arrows (e to f and h to i) indicate that the 70°C FISH is followed by the 95°C FISH.

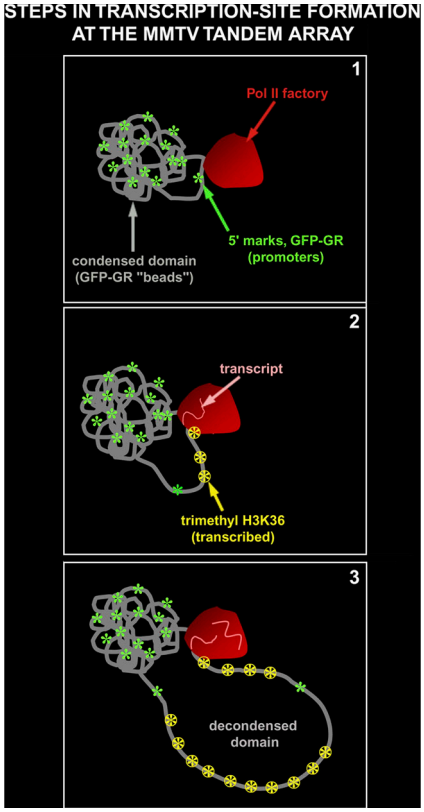


Figure 8. **A model for patterns of chromatin organization and histone modifications at the MMTV tandem array.** Upon hormone stimulation, GFP-GR binds to MMTV promoters within the condensed domain, thereby defining the GFP-GR beads visible in live cells. Some of these GFP-GR–bound promoters associate with transcription factories (step 1). A polymerase within the factory transcribes the downstream reporter sequence, extruding it into the surroundings with multiple trimethyl H3K36 marks attached (step 2). The tandem nature of the array promotes iteration of this process, thereby giving rise to large decondensed domains easily visible by light microscopy (step 3). Promoter marks (green) are enhanced within the condensed domain as a result of the density of chromatin there, but the trimethyl H3K36 mark is not detectable there (Fig. 5, b–d), suggesting that transcribed sequences are not found in the condensed domain. Rather, these transcribed marks are found only in the decondensed domain, which extends well beyond the sites of transcription, implying that the transcribed sequences are extruded from the transcription site.

within the GFP-GR beads. All of these marks for promoters, including GFP-GR, are probably higher within the GFP-GR beads because the chromatin concentration is substantially higher there than in the decondensed domain (approximately seven times more based on our rough estimate). We could find no evidence for the alternate possibility that promoter sequences are preferentially enriched within the beads because DNA FISH with a promoter-specific probe demonstrated that promoter sequences were present not only in the GFP-GR beads but also in the decondensed domain.

Despite the increased chromatin concentration within GFP-GR beads leading to the enhancement of 5′ marks there, no such enhancement was detected for the 3′ trimethyl H3K36 mark. However, DNA FISH with a reporter probe showed that reporter sequences were also present within both the GFP-GR beads and the surrounding decondensed domain. Thus, the lack of trimethyl H3K36 staining in the GFP-GR beads indicates that the reporter sequences within this condensed domain have not been transcribed. Because multiple trimethyl H3K36 marks are placed on each segment of transcribed chromatin, the substantial enhancement of this mark relative to any other histone modification in the decondensed domain is expected if this domain contains recently transcribed chromatin.

Together, these results suggest a model for transcription site formation at the MMTV array (Fig. 8). Promoter regions within the condensed domain are bound by GFP-GR, resulting in its visibility within live cells as the GFP-GR beads. Some of these GFP-GR–bound promoters then associate with pol II transcription factories. This leads to production within the pol II factory of nascent transcripts from the downstream reporter gene accompanied by deposition of the trimethyl H3K36 mark at multiple sites along the reporter gene. The transcribed sequences are extruded from the pol II factory, producing the decondensed domain and an enrichment of the trimethyl H3K36 mark in this region. The tandem nature of the gene array favors iteration of this process at consecutive promoters, thereby leading to a large decondensed domain visible by light microscopy.

### Limitations of this study and future prospects

Our conclusions here are based on the premise that the array exploits the normal cellular transcription machinery, thereby yielding structural features at a transcription site that are amplified versions of those that occur at endogenous loci. Considerable biochemical evidence indicates that transcription occurs normally from the array, and further evidence suggests that the bead chromatin structure of the array also occurs in natural chromatin (see Introduction). However, the sequence composition at endogenous loci is less gene dense and more complex than the simple, repetitive nature of the array. Whether endogenous genes exhibit comparable decondensed domains can now be assayed using the new, gentler DNA FISH that we have developed here. Although we would predict that decondensed domains at endogenous loci should be considerably smaller, some may still be detectable by light microscopy if long transcripts are encoded.

Although our results provide new structural evidence for the immobilized pol II factory model, they do not provide definitive proof that transcripts actually move rather than the polymerase. This might be tested directly in the future if in vivo marks for the decondensed chromatin domain can be developed enabling time-lapse 3D imaging to assess whether chromatin within the decondensed domain moves in and out of the pol II transcription site.

In summary, we have identified a new decondensed chromatin domain surrounding transcription factories. This domain requires transcription for its formation and shows enrichment for a histone modification that is characteristic of recently transcribed chromatin. These observations provide new support for the immobilized pol II factory model and, in addition, suggest further tests of this model at both the tandem array and endogenous loci.

## Materials and methods

#### Cell culture

The MMTV array cell line (3617) was grown as previously described (Müller et al., 2001). For microscopy experiments, cells were grown on #1.5 coverslips. To induce GR-mediated transcription from the MMTV array, 100 nM dexamethasone was added to cells for 0.5–1.5 h.

#### BrUTP incorporation

The protocol followed that in Elbi et al. (2002), with the following modifications. The permeabilization buffer contained 25 μg/ml instead of 5 μg/ml digitonin, 1 mM PMSF instead of 0.5 mM PMSF, and 100 nM dexamethasone. The transcription buffer contained 10 mM $MgCl_2$ instead of 5 mM, and the transcription reaction was run for 15 min at room temperature.

#### Immunofluorescence

Cells were fixed in either 3.5% PFA in PBS for 20 min followed by 0.5% Triton X-100 in PBS for 10 min or in 0.5% formaldehyde in PEM buffer (100 mM Pipes, 5 mM EGTA, 2 mM $MgCl_2$, pH 6.8, and 0.2% Triton X-100) for 5 min. The former fix tended to give more intense staining patterns for markers associated with the GFP-GR beads, whereas the latter fix tended to give more intense staining patterns for markers associated with the decondensed domain, although the pattern of staining itself was not dependent on the fixation protocol. Before antibody incubation, cells were washed three times for 10 min each in PBS.

The primary antibodies used were as follows: anti-BrdU mouse monoclonal (Caltag) or anti-BrdUTP rat monoclonal (Oxford Biotechnology); anti–topoisomerase IIα (Topogen); anti–pol II H5 (Covance); anti–human Set2 orthologue (HYPB) N terminus (Abgent); anti–trimethyl H3K36, anti–acetyl H4, and anti–acetyl H3K9 (Upstate Biotechnology); and anti–trimethyl H3K4 (Abcam).

The secondary antibodies used were as follows: Texas red–conjugated anti–mouse and anti–rabbit, rhodamine-conjugated anti–rat (Rockland), and Cy5-conjugated anti–mouse (Jackson ImmunoResearch Laboratories). Antibodies were diluted in PBS with 4% BSA and 0.1% Tween 20. Primary antibodies were incubated overnight at 4°C. After incubation, washes were performed three times with PBS for 20–30 min total. In some cases, the first wash also contained 0.1% Tween, and the incubation time was reduced to 5 min. Secondary antibodies were incubated from 40–60 min at room temperature and washed three times in PBS for a total of 20 min.

#### Array-specific DNA FISH

**Decondensed domain–specific fixation and denaturation.** Cells were fixed for 30 min by adding an equal volume of 7.0% PFA in PBS to the DME culture media. Improved staining was often achieved when this fix was preceded by a 5-min prefix in 0.5% formaldehyde in PEM buffer. Cells were then washed three times with PBS for 10 min each, permeabilized for 10 min with 0.5% Triton X-100 in PBS, and washed with PBS again. Then, cells were incubated in 50 μg/ml RNase for 30–60 min and washed three times in PBS for 10 min each. DNA was denatured by incubation at 70°C for 10 min in 70% formamide in 2× SSC followed by dehydration for 2–5 min each in 70, 90, and 100% ethanol kept on ice.

**Condensed domain–specific fixation and denaturation.** This was identical to the decondensed domain protocol described in the previous paragraph except that cells were fixed for 30 min with the 3.5% PFA fix described above, and denaturation was performed for 5 min at 95°C.

**Probe preparation and hybridization.** Three types of probe-specific DNA were used: array, promoter, and reporter. The array-specific probe was prepared as previously described (Müller et al., 2001), but with the following modifications: the biotin and digoxigenin nick translation mix was purchased from Roche, and the entire pM18 plasmid (Ostrowski et al., 1983) was used as a template. The promoter-specific probe was a 1.9-kb BstX1–BamH1 fragment of the pM18 plasmid. The reporter-specific probe was a 2-kb BamH1–Sal1 fragment of the pM18 plasmid. Hybridization was also performed essentially as previously described (Müller et al., 2001) except that the dextran sulfate concentration of the hybridization mix was reduced to 5%. The hybridized probe was detected as follows: for condensed domain FISH, probes were detected with streptavidin AlexaFluor488 (Invitrogen), whereas for decondensed domain FISH, probes were detected with an antidigoxigenin (sheep) primary antibody (Roche) followed by an AlexaFluor594-conjugated anti–sheep secondary antibody (Invitrogen).

**Double FISH.** The first stage of this protocol followed that for the decondensed domain–specific fixation and denaturation procedure, and the detection protocol for this first stage followed that for probe preparation and hybridization. Then, cells were fixed a second time for 15–20 min in 3.5% PFA in PBS, washed in PBS, permeabilized for 10 min in 0.5% Triton X-100, and washed with PBS again. DNA was then denatured for the second time according to the condensed domain–specific fixation and denaturation protocol. The second detection step followed that for aforementioned probe preparation and hybridization.

#### RNA FISH

RNA FISH was performed as previously described (Müller et al., 2001) except that cells were fixed for 30 min with 3.5% PFA in PBS, and the hybridized probe was detected with streptavidin AlexaFluor488 (Invitrogen).

#### Drug inhibition experiments

**DRB.** Transcription was induced with 100 nM dexamethasone, and DRB (Calbiochem) was added simultaneously at 100 μg/ml (from a 1-mg/ml stock solution in water dissolved by heating). After a 45-min incubation, the cells were prepared for decondensed domain–specific FISH.

**Etoposide.** Transcription was induced with 100 nM dexamethasone, and etoposide (Sigma-Aldrich) was added simultaneously at 250 μM (from a 500-mM stock solution in DMSO). After a 45-min incubation, the cells were prepared for decondensed domain–specific DNA FISH. The same protocol was used for RNA FISH measurements.

#### Microscopy

Images of BrUTP incorporation and active pol II were obtained by 3D deconvolution microscopy of PFA-fixed specimens mounted in PBS. Images were collected with a CCD camera (CoolSNAP HQ; Photometrics) mounted

on a microscope (IX70; Olympus) equipped with a 100× 1.35 NA oil immersion objective (Olympus). Voxel sizes were set at 0.07 × 0.07 × 0.07 μm with 16–32 focal planes. Images were collected and also preprocessed to correct for photobleaching using the softWoRx package (Applied Precision), and the maximum likelihood algorithm from the publicly available XCOSM software was run for 200 iterations.

For colocalization analysis, these deconvolved images were corrected for chromatic aberration. This was calibrated by imaging a 0.5-μm TetraSpeck multicolored fluorescent bead (Invitrogen). Using this bead, we found that xy shifts from the GFP channel to the Texas red channel were less than a pixel (0.07 μm) and so were not corrected, but a z shift of approximately two focal planes (0.14 μm) was present and subsequently corrected.

Immunofluorescence images of histone modification patterns were collected with a spinning disk confocal microscope (Ultraview LCI CSU10; PerkinElmer) mounted on a microscope (Axiovert 200; Carl Zeiss MicroImaging, Inc.) equipped with a 63× 1.4 NA objective.

DNA FISH images were acquired on an upright microscope (DMRA; Leica) with a 100× 1.3 NA oil-immersion objective (Leica). Images were obtained with a CCD camera (Sensys; Roper Scientific).

All specimens were mounted in PBS for imaging. Images were cropped within MetaMorph software (Molecular Devices). Overlay images were generated using Imaris (Bitplane AG). Figures were assembled in Photoshop (Adobe), in which contrast adjustments were also performed by setting minimum and maximum intensity values in each color and displaying a linear contrast range between these endpoints.

### Image measurements

All image measurements were performed with MetaMorph software (Molecular Devices). RNA FISH intensities and mean areas of structures were determined as previously described (Müller et al., 2001).

### ChIP and real-time PCR

Cells were treated with either vehicle or 100 nM dexamethasone for 60 min and were processed for ChIP using a ChIP assay kit (Upstate Biotechnology). In brief, cells were cross-linked for 10 min at 37°C in 0.5% formaldehyde followed by a quenching step for 10 min with 150 mM glycine. Soluble chromatin was immunoprecipitated with an antibody to a trimethyl H3K36 mark (Upstate Biotechnology) with 12 μl of antibody per reaction. DNA isolates from immunoprecipitates were used as templates for real-time quantitative PCR amplification.

Real-time assays were conducted on a real-time detection system (iCycler IQ; Bio-Rad Laboratories) using the intercalation dye SYBR green as the fluorescence agent (iQ SYBR Green Supermix; Bio-Rad Laboratories) and the manufacturer's recommended conditions. PCR was performed by denaturing at 95°C for 15 s and annealing/extending at 60°C for 60 s. Standard curves were created for each run using a plasmid (pM18) that contained the MMTV long terminal repeat and primers that spanned either the promoter or reporter regions of the MMTV array. 10-fold serial dilutions of pM18 (over three logs) were used to generate the standard curve. All PCR reactions were subjected to a melting curve to verify the integrity of the PCR product and to eliminate amplification of nonspecific products. The following primers were used for amplification: promoter primers, sense (5′-TTTCCATACCAAGGAGGGGACAGTG-3′) and antisense (5′-CTTACTTAAGCCTTGGGAACCGCAA-3′); reporter primers, sense (5′-CGTGAGATTCGGCAGCATAAA-3′) and antisense (5′-GACAGCACACACTTGCAGCTC-3′).

In each of the ChIPs, all Ct (threshold cycle) values were normalized to promoter primers with no antibody. The fold enrichment at the reporter or promoter was then calculated by dividing each immunoprecipitation value by the respective no-antibody value. Both reporter and promoter primers amplified input (genomic) DNA with similar efficiencies.

### Online supplemental material

Fig. S1 shows immuno-FISH at 95°C with a GR antibody. Fig. S2 shows 70°C FISH controls (no probe DNA or 95°C pretreatment). Online supplemental material is available at http://www.jcb.org/cgi/content/full/jcb.200703157/DC1.

We are grateful to Dr. Valarie Barr for use of the Laboratory of Cellular and Molecular Biology microscopy core and thank Dr. Keji Zhao for comments on the manuscript.

This work was supported by the intramural program of the National Institutes of Health, National Cancer Institute, Center for Cancer Research, the Human Frontier Sciences Program, the Genome Research in Austria project Bioinformatic Integration Network, and the Austrian Ministry for Education, Science, and Culture.

Submitted: 26 March 2007
Accepted: 17 May 2007

## References

Bannister, A.J., R. Schneider, F.A. Myers, A.W. Thorne, C. Crane-Robinson, and T. Kouzarides. 2005. Spatial distribution of di- and tri-methyl lysine 36 of histone H3 at active genes. *J. Biol. Chem.* 280:17732–17736.

Becker, M., C. Baumann, S. John, D.A. Walker, M. Vigneron, J.G. McNally, and G.L. Hager. 2002. Dynamic behavior of transcription factors on a natural promoter in living cells. *EMBO Rep.* 3:1188–1194.

Bernstein, B.E., M. Kamal, K. Lindblad-Toh, S. Bekiranov, D.K. Bailey, D.J. Huebert, S. McMahon, E.K. Karlsson, E.J. Kulbokas III, T.R. Gingeras, et al. 2005. Genomic maps and comparative analysis of histone modifications in human and mouse. *Cell*. 120:169–181.

Chakalova, L., E. Debrand, J.A. Mitchell, C.S. Osborne, and P. Fraser. 2005. Replication and transcription: shaping the landscape of the genome. *Nat. Rev. Genet.* 6:669–677.

Chodosh, L.A., A. Fire, M. Samuels, and P.A. Sharp. 1989. 5,6-Dichloro-1-beta-D-ribofuranosylbenzimidazole inhibits transcription elongation by RNA polymerase II in vitro. *J. Biol. Chem.* 264:2250–2257.

Cmarko, D., P.J. Verschure, T.E. Martin, M.E. Dahmus, S. Krause, X.D. Fu, R. van Driel, and S. Fakan. 1999. Ultrastructural analysis of transcription and splicing in the cell nucleus after bromo-UTP microinjection. *Mol. Biol. Cell*. 10:211–223.

Collins, I., A. Weber, and D. Levens. 2001. Transcriptional consequences of topoisomerase inhibition. *Mol. Cell. Biol.* 21:8437–8451.

Cook, P.R. 1995. A chromomeric model for nuclear and chromosome structure. *J. Cell Sci.* 108:2927–2935.

Cook, P.R. 1999. The organization of replication and transcription. *Science*. 284:1790–1795.

Elbi, C., T. Misteli, and G.L. Hager. 2002. Recruitment of dioxin receptor to active transcription sites. *Mol. Biol. Cell*. 13:2001–2015.

Fragoso, G., W.D. Pennie, S. John, and G.L. Hager. 1998. The position and length of the steroid-dependent hypersensitive region in the mouse mammary tumor virus long terminal repeat are invariant despite multiple nucleosome B frames. *Mol. Cell. Biol.* 18:3633–3644.

Hozak, P., P.R. Cook, C. Schofer, W. Mosgoller, and F. Wachtler. 1994. Site of transcription of ribosomal RNA and intranucleolar structure in HeLa cells. *J. Cell Sci.* 107:639–648.

Iborra, F.J., and P.R. Cook. 2002. The interdependence of nuclear structure and function. *Curr. Opin. Cell Biol.* 14:780–785.

Iborra, F.J., A. Pombo, D.A. Jackson, and P.R. Cook. 1996. Active RNA polymerases are localized within discrete transcription "factories" in human nuclei. *J. Cell Sci.* 109:1427–1436.

Jackson, D.A., A.B. Hassan, R.J. Errington, and P.R. Cook. 1993. Visualization of focal sites of transcription within human nuclei. *EMBO J.* 12:1059–1065.

Liang, G., J.C. Lin, V. Wei, C. Yoo, J.C. Cheng, C.T. Nguyen, D.J. Weisenberger, G. Egger, D. Takai, F.A. Gonzales, and P.A. Jones. 2004. Distinct localization of histone H3 acetylation and H3-K4 methylation to the transcription start sites in the human genome. *Proc. Natl. Acad. Sci. USA*. 101:7357–7362.

Liu, L.F., and J.C. Wang. 1987. Supercoiling of the DNA template during transcription. *Proc. Natl. Acad. Sci. USA*. 84:7024–7027.

McNally, J.G., W.G. Müller, D. Walker, R. Wolford, and G.L. Hager. 2000. The glucocorticoid receptor: rapid exchange with regulatory sites in living cells. *Science*. 287:1262–1265.

Mondal, N., Y. Zhang, Z. Jonsson, S.K. Dhar, M. Kannapiran, and J.D. Parvin. 2003. Elongation by RNA polymerase II on chromatin templates requires topoisomerase activity. *Nucleic Acids Res.* 31:5016–5024.

Morris, S.A., Y. Shibata, K. Noma, Y. Tsukamoto, E. Warren, B. Temple, S.I. Grewal, and B.D. Strahl. 2005. Histone H3 K36 methylation is associated with transcription elongation in *Schizosaccharomyces pombe*. *Eukaryot. Cell*. 4:1446–1454.

Müller, W.G., D. Walker, G.L. Hager, and J.G. McNally. 2001. Large-scale chromatin decondensation and recondensation regulated by transcription from a natural promoter. *J. Cell Biol.* 154:33–48.

Müller, W.G., D. Rieder, G. Kreth, C. Cremer, Z. Trajanoski, and J.G. McNally. 2004. Generic features of tertiary chromatin structure as detected in natural chromosomes. *Mol. Cell. Biol.* 24:9359–9370.

Osborne, C.S., L. Chakalova, K.E. Brown, D. Carter, A. Horton, E. Debrand, B. Goyenechea, J.A. Mitchell, S. Lopes, W. Reik, and P. Fraser. 2004. Active genes dynamically colocalize to shared sites of ongoing transcription. *Nat. Genet.* 36:1065–1071.

Ostrowski, M.C., H. Richard-Foy, R.G. Wolford, D.S. Berard, and G.L. Hager. 1983. Glucocorticoid regulation of transcription at an amplified, episomal promoter. *Mol. Cell. Biol.* 3:2045–2057.

Pokholok, D.K., C.T. Harbison, S. Levine, M. Cole, N.M. Hannett, T.I. Lee, G.W. Bell, K. Walker, P.A. Rolfe, E. Herbolsheimer, et al. 2005. Genome-wide map of nucleosome acetylation and methylation in yeast. *Cell*. 122:517–527.

Roh, T.Y., S. Cuddapah, and K. Zhao. 2005. Active chromatin domains are defined by acetylation islands revealed by genome-wide mapping. *Genes Dev.* 19:542–552.

Schneider, R., A.J. Bannister, F.A. Myers, A.W. Thorne, C. Crane-Robinson, and T. Kouzarides. 2004. Histone H3 lysine 4 methylation patterns in higher eukaryotic genes. *Nat. Cell Biol.* 6:73–77.

Strahl, B.D., P.A. Grant, S.D. Briggs, Z.W. Sun, J.R. Bone, J.A. Caldwell, S. Mollah, R.G. Cook, J. Shabanowitz, D.F. Hunt, and C.D. Allis. 2002. Set2 is a nucleosomal histone H3-selective methyltransferase that mediates transcriptional repression. *Mol. Cell. Biol.* 22:1298–1306.

Sun, X.J., J. Wei, X.Y. Wu, M. Hu, L. Wang, H.H. Wang, Q.H. Zhang, S.J. Chen, Q.H. Huang, and Z. Chen. 2005. Identification and characterization of a novel human histone H3 lysine 36-specific methyltransferase. *J. Biol. Chem.* 280:35261–35271.

Toohey, M.G., J.W. Lee, M. Huang, and D.O. Peterson. 1990. Functional elements of the steroid hormone-responsive promoter of mouse mammary tumor virus. *J. Virol.* 64:4477–4488.

Vakoc, C.R., M.M. Sachdeva, H. Wang, and G.A. Blobel. 2006. Profile of histone lysine methylation across transcribed mammalian chromatin. *Mol. Cell. Biol.* 26:9185–9195.

Verschure, P.J., van Der Kraan, E.M. Manders, and R. van Driel. 1999. Spatial relationship between transcription sites and chromosome territories. *J. Cell Biol.* 147:13–24.

Walker, D., H. Htun, and G.L. Hager. 1999. Using inducible vectors to study intracellular trafficking of GFP-tagged steroid/nuclear receptors in living cells. *Methods*. 19:386–393.

Wansink, D.G., O.C. Sibon, F.F. Cremers, R. van Driel, and L. de Jong. 1996. Ultrastructural localization of active genes in nuclei of A431 cells. *J. Cell. Biochem.* 62:10–18.